Analysis of the Effect of Circular Ring Baffles in Suppressor on Flow Field and Far Field Noise Levels at 9 mm Semi-Automatic Pistol

Onur Gurdamar [#], Seyda Ozbektas[$] and Bilal Sungur [#,*]

[#]*Department of Mechanical Engineering, Samsun University, Samsun, Turkey*
[$]*Department of Mechanical Engineering, Ondokuz Mayis University, Samsun, Turkey*
E-mail: bilal.sungur@samsun.edu.tr

ABSTRACT

A firearm generates complex phenomena in muzzle flow and modelling the flow field around the projectile has great importance on high-intensity noise prediction. The negative effects of noise can be reduced using a suppressor which can be internally or externally attached to the barrel of a firearm. The purpose of this paper is to numerically and experimentally investigate the effect of the number and distance of circular ring baffles in the suppressor on the flow field and far field noise levels. Calculations were carried out in two-dimensional, axisymmetric, transient conditions and Ffowcs Williams and Hawkings acoustic analogy (FW-H) equations were solved to predict the far field noise. Nine cases including a gun without a suppressor, a suppressor without baffles, one, three, and five baffles which were placed at 20 mm intervals from the suppressor inlet, and one, three, five, seven, and nine baffles which were placed with equal intervals in the suppressor were simulated and compared; generations of noise during the shooting process were analyzed. The results showed that in the case without a suppressor, the peak sound pressure level was 156.1 dB at a 2.5 m distance, while this value decreased by nearly 7.6% in the case of the suppressor with seven baffles which has an average value of 144.2 dB. The results obtained here may provide a beneficial reference for predicting the muzzle noise and optimizing the number of baffles in the suppressor for small caliber gun systems.

Keywords: Firearm; Muzzle flow field; Sound pressure; Suppressor; Numerical simulation

NOMENCLATURE

a_0 : Sound speed in the fluid medium
F : Body force
$H(f)$: Heaviside function
p : Instantaneous pressure
p_0 : Atmospheric pressure
p' : Sound pressure
P_{ij} : Compressive stress tensor
p_{ref} : Minimum threshold of sound that a human can hear
Q : Mass source in the continuity equation
T_{ij} : Lighthill stress tensor
u_i : Fluid velocity components in the x_i direction
u_n : Fluid velocity components in the direction normal to the acoustic surface
v_n : Surface velocity component normal to the acoustic surface
$\delta(f)$: Dirac delta function
ρ : Density

1. INTRODUCTION

High-intensity noise occurs in form of muzzle blast waves when the gun is fired. Basically, three main sources of noise occurred while firing a gun: muzzle blast (impulse), sonic boom (bow shock) and mechanical noises from internal moving parts. Impulse noise is a transient noise which occurs when the projectile uncorks the high-pressure propellant gases. It is caused by many factors such as turbulent fluctuation in the mixing zone of the expanded jet at high speeds or the unstable shock wave in muzzle flow mostly, and dependent on the geometry and scale of the source[1-2]. A sound suppressor is attached to the barrel of the firearm in order to reduce the sound and explosion of a firearm. It is generally known that the increasing the length of the suppressor not only reduces noise exposure but also reduces recoil and even improves accuracy for any given cartridge of the weapons[3]. There are different number of expansion chambers created by using a series of baffles inside the suppressor[4].

To understand the mechanism of muzzle flow fields and to see the effect of projectile motion on the flow field and noise levels, great effort has been made. Luo[5], *et al.* numerically calculated the dynamic processes during the projectile launched from the barrel of a gun into the ambient air. Trabinski[6], *et al.* investigated the effect of muzzle device on the flow field around a projectile. Jiang, Z.[7], *et al.* researched the jet-flow and shock-wave interactions created by a flat-nosed supersonic projectile released into ambient air. Kikuchi[8], *et al.* experimentally and numerically analyzed the bow shock wave mechanism occurred in front of the projectile[9], *et al.* numerically researched

Table 1. Noise reduction performances of different suppressor models

Gun Type	Bullet diameter (mm)	Supressor model	Distance (m)	Noise reduction (dB)	Suppressed SPL$_{peak}$ (dB)	Reference
Pistol	9		0*	23.5	140.4	
Pistol	9		0*	22.3	140.9	
Pistol	11.43		0*	19	146.6	22
Rifle	5.56		0*	19.3	126.1	
Rifle	5.56		4	~13	~145	11
Rifle	7.62		4	~16	~147	
Rifle	7.62		4	~16	~147	4
Rifle	7.62		4	~16	~147	
Tank	120		4	16	242	14

*The microphone is positioned in line with the shooter and 15 cm to the left of the shooter.

decreasing the noise levels for a high pressure explosion from a shock tube to the surrounding environment. Xavier[10] analysed the effect of projectile mass, pressure and temperature on the pressure and sound distribution at firearm.

Huerta-Torres[11], *et al.* experimentally and numerically investigated the effect of a sound suppressor for a 5.56 mm caliber rifle. Their numerical results showed an average value of 143 dB for the considered three model configurations with curved deflectors, conical deflectors, and with a reactive spiral. Hudson[12], *et al.* designed a model suppressor and carried out experiments and simulations and examined the accuracy of the computational models. They observed that simulations can accurately predict acoustic signal produced by the bare barrel and suppressor configurations. Paakonen[13], *et al.* researched the noise reduction of weapons by changing the frequency of gunshot noise.

Rehman[14], *et al.* used three baffle silencer during high pressure blast flow at large caliber 120 mm K1A1 tank gun. They obtained approximately 90 % of pressure and 20 dB of sound level decrease at the muzzle end of the gun barrel with using three baffle silencers. Murphy[15], *et al.* focused on reduction of peak levels, equivalent energy and sound power of firearm suppressors. They found that suppressors reduced the measured sound power levels in the range of 2 and 23 dB. Lobarinas[16], *et al.* investigated the performance of several suppressors at semi-automatic rifles. They reported that the sound attenuation varied with the suppressor type and the

measurement location. Also, they stated that nearly 20 dB and 30 dB of peak reduction occurred with suppressor usage for the muzzle. Nakashima[17] realised a series of measurements by using small-caliber firearms with and without suppressors. Their results showed that at 0.5 to 1 m to the side of the shooter, the peak sound levels reduced by 22 dB at 5.56 mm C8 semi-automatic rifle.

There are limited studies in literature on the calculation and prediction of the muzzle noise field especially far field noise due to the complex structure of flow field. The experiments do not allow instantaneous changes in the flow field to be seen and do not show the propagation of the muzzle noise field caused by the firing of the gun. Additionally, gun testing in both near and far flow fields is very expensive and time-consuming. The flow field near the muzzle can be simulated with Computational Fluid Dynamics (CFD) programs and it can easily predict the noise, but it is not sufficient for predicting the far field noises. In this context computational fluid dynamics (CFD) - computational aeroacoustic (CAA) hybrid methods was an alternative approach and investigated by many researchers[2,18-21]. Zhao[2], *et al.* investigated the impulse noise caused by complex jet streams from muzzle suppressor small-bore rifles. They observed that the muzzle suppressor changed the flow area and the directional distribution of the sound. Jonghoon[18], *et al.* numerically investigated the impulse noise produced by complex flows discharged from a barrel in a two-dimensional axisymmetric solution. They discussed the

complex flow properties and noise generation mechanisms around the muzzle. They stated that numerical simulation using computational aeroacoustic (CAA) methods not only provides a reliable way to determine the blast wave dynamics of muzzle flow, but also provides an opportunity to examine the physics and detailed mechanisms of noise generation and propagation due to interaction. Lee[19], *et al.* calculate the noise field with and without silencers using CFD-CAA coupled method at two dimensional conditions. Wang[20], *et al.* used CAA by using FW-H equation and determined the noise discharging directivity of small caliber rifle. Zhao[21], *et al.* used CFD-CAA coupled method while evaluating the performance of muzzle brake targeting efficiency and impulse noise.

The noise reduction performances of different suppressor models were given in Table 1 in order to better understand the effect of the suppressor geometries on the peak sound pressure level (SPL_{peak}).

The majority of the studies in the literature are related to rifle shooting and the design of muzzle brake to reduce the sound intensity at the time of the explosion and their effect on the flow around the barrel. However, in most studies, the effect of the projectile on the flow field and the noise after the explosion was analyzed separately. Also, there are very limited studies on determining the optimum number of baffles to be placed in the suppressor. The main aim of this study is to fill these gaps in the literature. In this context, the effect of the number and distance of the baffles in the suppressor on the flow field and sound pressure level (SPL) was investigated numerically and experimentally. The numerical model was validated with a 9x19 mm semi-automatic pistol without a suppressor using a subsonic projectile and the SPL_{peak} values were taken from the study of Gürdamar[23], *et al.* In the study of Gürdamar[23], *et al.*, the SPL_{peak} values after firing the subsonic and supersonic projectiles from a 9 mm semi-automatic pistol without a suppressor were experimentally measured at different distances. After the validation, a suppressor without baffles was first modelled. Then, one, three, and five baffles were placed at 20 mm intervals from the suppressor inlet and these four models were calculated numerically. In addition to these models, the effect of one, three, five, seven, and nine baffles, which were placed with equal intervals in the suppressor, on the SPL_{peak} was investigated both numerically and experimentally.

2. METHODOLOGY
2.1 Experimental Setup

Gunshots were conducted in outdoor. The experimental setup basically consisted of a 9x19 mm semi-automatic pistol (Canik TP9 Elite Combat model), table, gun stabilizer, Larson Davis LXT sound level meter, and Labradar Ballistic Velocity Doppler Radar Chronograph. The gun was fixed to a gun stabilizer which was above 1 m from the ground to prevent the sound reflection. Subsonic projectiles were used in gunshot tests. The microphone was mounted on a tripod vertically, and the height of the tripod was in level with the gun barrel axis in all experiments. The gun was fired six times at intervals of 10 seconds for each point where the SPL_{peak} value was measured. Before starting the tests, the microphone calibration was tested using the CAL200 sound level calibrator. The minimum

SPL_{peak} value was obtained numerically in Case 5 which is in the first configuration cases. In this context, experiments were made with first configuration cases. Therefore, experiments were carried out for five cases including one, three, five, seven, and nine baffles which were placed with equal intervals inside the suppressor. The schematic and real time illustration of the experimental setup is given in supplementary files. Also, the details of the experiments can be found in[23], except gunshots with suppressors.

2.2 Numerical Method
2.2.1 FW-H Acoustic Model

Noise in firearms is generally caused by strong vortices and shock waves radiating from the muzzle. When a gun is fired, the unstable flow field occurs at the barrel exit due to the effect of high pressure and temperature. Additionally, the energy of this flow field is much higher than the sound energy. These situations make it difficult to calculate the sound waves numerically. Ansys fluent presents a hybrid method that allows Computational Fluid Dynamic (CFD) and Computational Aeroacoustics (CAA) to be analyzed together. Aerodynamic acoustics are developed using the Lighthill acoustic analogy equation obtained by rearranging the mass and momentum equations[24]. In this equation, the sound source term is derived from the Navier-Stokes equations. The Lighthill equation was given in Eqn. (1).

$$\frac{\partial^2 \rho}{\partial t^2} - a_0^2 \nabla^2 \rho = \frac{\partial Q}{\partial t} - \nabla F + \frac{\partial^2 (T_{ij})}{\partial x_i x_j} \tag{1}$$

In Eq. (1), Q and a_0 correspond the mass source in the continuity equation and the sound speed in the fluid medium, respectively. F and T_{ij} represent the body force and the Lighthill stress tensor, respectively.

In this study, the Ffowcs Williams and Hawkings Acoustics Model was used to compute the far field noise. In this model, sound pressure signals are calculated simultaneously at prescribed receivers. The FW-H equation is derived from Lighthill's acoustic analogy. It is an inhomogeneous wave equation that takes into account the presence of an impermeable surface in the flow. This equation consists of three inhomogeneous terms: monopole, dipole and quadrupole. Monopole acoustic source is one source originating from unsteady mass injection. Dipole acoustic source is two monopole sources originating from unsteady external forces. Quadrupole acoustic source is two dipole sources originating from unsteady shear stresses. The monopole and dipole terms together represent the sound generated by the body passing through the flow[24]. The FW-H equation is given in Eqn. (2).

$$= \frac{1}{a_0^2} \frac{\partial^2 p'}{\partial t^2} - \nabla^2 p'$$

$$\frac{\partial^2}{\partial x_i \partial x_j} \{ T_{ij} H(f) \} (\text{monopole})$$

$$\frac{-\partial}{\partial x_i} \{ [P_{ij} n_j + \rho u_i (u_n - v_n)] \delta(f) \} (\text{dipole}) \tag{2}$$

$$\frac{+\partial}{\partial t} \{ [\rho_0 v_n + \rho (u_n - v_n)] \delta(f) \} (\text{quadrupole})$$

$$T_{ij} = \rho u_i u_j + P_{ij} - a_0^2 (\rho - \rho_0) \delta(f) \tag{3}$$

$$P_{ij} = \rho \delta_{ij} - \mu \left[\frac{\partial u_i}{\partial x_j} + \frac{\partial u_j}{\partial x_i} - \frac{2}{3} \frac{\partial u_k}{\partial x_k} \delta_{ij} \right] \tag{4}$$

In Eq. (2), the acoustic source surface is defined as $f = 0$. u_i represents fluid velocity components in the x_i direction, u_n in the direction normal to the acoustic surface. v_n expresses the surface velocity component normal to the acoustic surface. $H(f)$ and $\delta(f)$ correspond to Heaviside and Dirac delta functions, respectively. Sound pressure is the difference between the instantaneous pressure at a point where a sound wave is present and the atmospheric pressure in the environment. It is defined as $p' = p - p_0$. In Eqns. (3) and (4), T_{ij} and P_{ij} express the Lighthill stress tensor and the compressive stress tensor, respectively.

Sound pressure level (SPL) is a logarithmic (decibel) measurement of sound pressure relative to the hearing threshold reference value. It is calculated according to the formula in Eq (5). P_{ref} is usually 2×10^{-5} Pa, which is the minimum threshold of sound that a human can hear.

$$SPL = 20 \log \frac{p'}{P_{ref}} \tag{5}$$

2.2.2 Boundary Conditions

In this section, the details related to numerical modelling of a gun with different suppressor models were given. The numerical model was validated according to a 9 mm semi-automatic pistol without a suppressor. The SPL_{peak} values were taken from the study of Gürdamar[23], et al. After the validation, a suppressor without baffles was first modelled. Then, 1, 3, and 5 baffles were placed at 20 mm intervals from the suppressor inlet. In addition to these models, the effect of 1, 3, 5, 7, and 9 baffles on the SPL_{peak} was investigated, which were placed evenly spaced in the suppressor. The flow events that occur in the near-field as a result of the firing of the gun were resolved using the fluent package program. Spalart-Allmaras was employed as the turbulence model. Air was defined as the gas in the cartridge. Soave Redlich Kwong real gas model was selected for air density. The cartridge pressure and temperature that accelerate the projectile were determined according to the factory data. In this context, the cartridge region was patched as 1600 atm and 1800 K. External ambient pressure and temperature were determined as 1 atm and 300 K, respectively. The no-slip condition was adopted for zero velocity at these wall boundaries. The pressure inlet boundary condition was adopted on the left side of the external ambient, and the total pressure and temperature were set to 1 atm and 300 K, respectively. On the other hand, the right and upper sides of the external ambient were defined as the pressure outlet, and the outlet pressures were set to 1 atm. Wall boundary condition was adopted on the projectile, barrel, and suppressor boundaries. The boundary conditions adopted in the numerical model were given in Fig. 1. In the fluent, the solution was performed in density-based, time-dependent, and two-dimensional axisymmetric conditions. Implicit formulation was employed as the solution method, and Advection Upstream Splitting Method (AUSM) was selected as the flow type. Flow evolutions that occur with the movement of the projectile were investigated in the 0.005 ms time interval. Accordingly, the frequency value reached 500000 in acoustic analysis. The step interval was set to 20 iterations, and the convergence criterion was defined as 10-3 for all Eqns.

In the FW-H acoustic model, three circular sound sources were placed external ambient to calculate the noise generated during the firing of the gun. Flow and acoustic analyze were initiated simultaneously. The receivers were placed to correspond to the measurement locations as in the study of Gürdamar[23], et al. In this context, the receivers were placed at 2.5 m, 5 m, 10 m, 20 m and 30 m distances from the barrel exit. The distances of all receivers from x-axis were 0.2 m.

2.2.3 Geometry

The geometry consisted of the dynamic field in which the projectile moved and the external ambient surrounding this field. In this context, a geometry without suppressor was first modelled to compare the numerical results with the experimental measurements. Then the geometries with suppressor were created. Within the scope of the study, the baffles in the suppressor were investigated in two configurations. In the first configuration cases, the baffles were placed evenly spaced in the suppressor, and one, three, five, seven, and nine baffles were used in the suppressor. In the second configuration cases, the baffles were placed in the suppressor at 20 mm intervals from the suppressor inlet, and one, three, and five baffles were used in the suppressor. In both configuration cases, the distance between the baffles was the same in the suppressor with 5 baffles. Therefore, case 4 is same for these two configurations. In addition to these models, a suppressor without baffles was also modelled. A total of nine different suppressors were modelled according to the number and distance of the baffles.

Since the barrel and projectile were in a symmetrical structure, the geometry was drawn as two-dimensional and
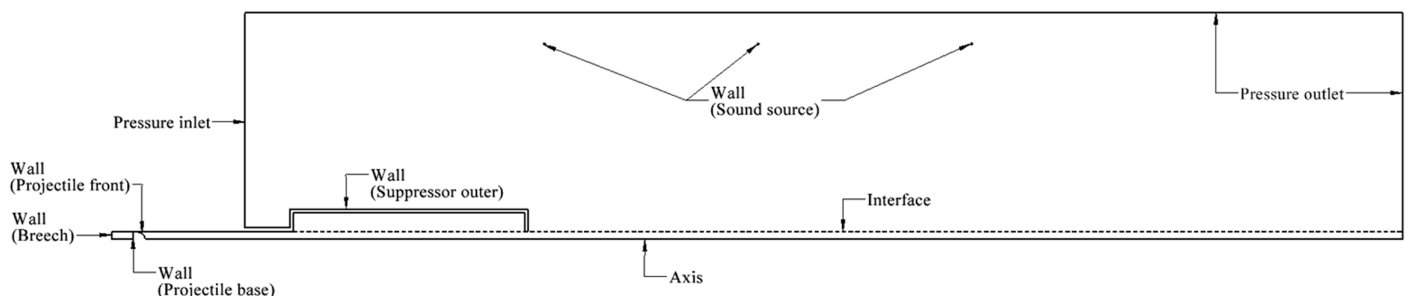

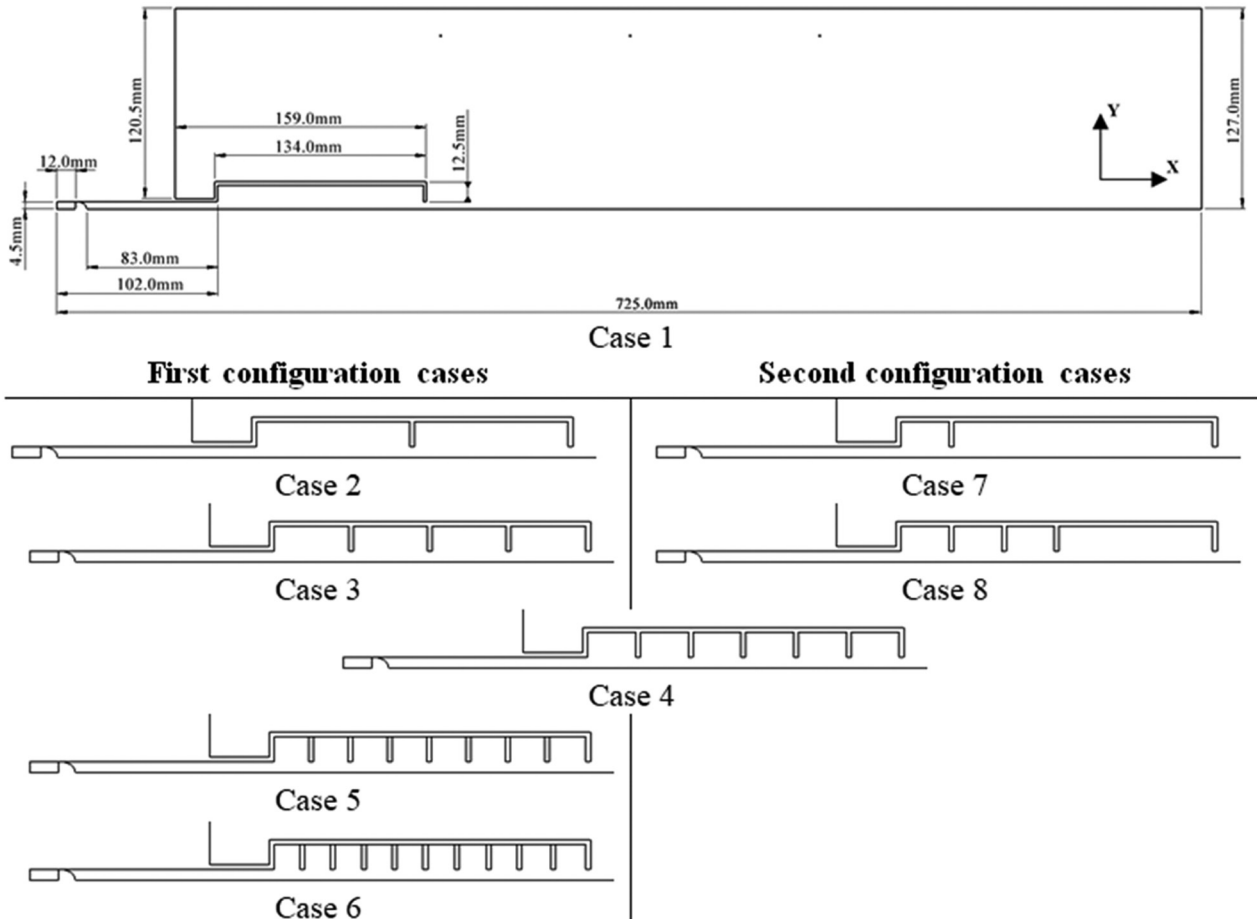**Figure 1. Boundary conditions adopted in numerical model.**

Figure 2. Schematic view of geometries used in numerical analyses.

axisymmetric. The calculation field had a length of 725 mm and a width of 127 mm. The diameter of the barrel and projectile was 9 mm and their length was 81 mm and 7 mm, respectively. The length and diameter of the suppressor were 130 mm and 30 mm, respectively. The wall thickness of the barrel, the suppressor and baffles were 2 mm. The schematic views of the geometries used in numerical analyzes were given in Fig. 2. Three circular sound sources with a diameter of 1 mm were placed external ambient to convert the pressure fluctuation occurring at the barrel exit into sound signals.

2.2.4 Mesh Structure

In this study, the boundary conditions in the modelled geometries changed as the projectile moved. For this purpose, dynamic mesh was activated to model the boundary conditions that changed with the movement of the projectile along the barrel. The path in which the boundary conditions changed and the projectile moved was defined as rigid, and the external ambient surrounding this path, and inside the suppressor were defined as stationary. Six Degrees of Freedom (Six-DOF) was activated so that the projectile could move freely along the barrel. The base and front boundaries of the projectile in Six-DOF were defined as rigid. The projectile weight was entered as 0.0032897 kg. The layering method, in which cell layers adjacent to a moving border are added or subtracted depending on the height of the layer adjacent to the moving surface, was selected as the dynamic mesh method. For the stable operation
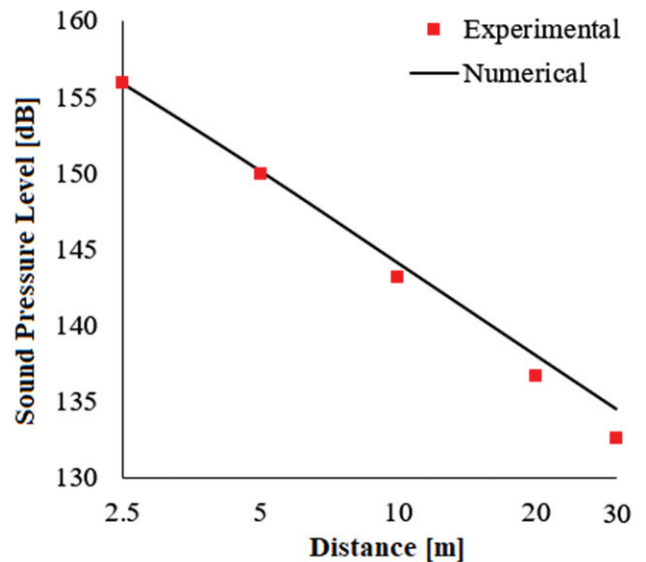

Figure 3. Comparison of experimental and numerical SPL$_{peak}$ values in a 9 mm semi-automatic pistol without a suppressor.

of this method, a rectangular mesh structure was used along the path of the projectile. In order to use different element types and sizes, the calculation field was divided into smaller fields and the details can be found in supplementary files.
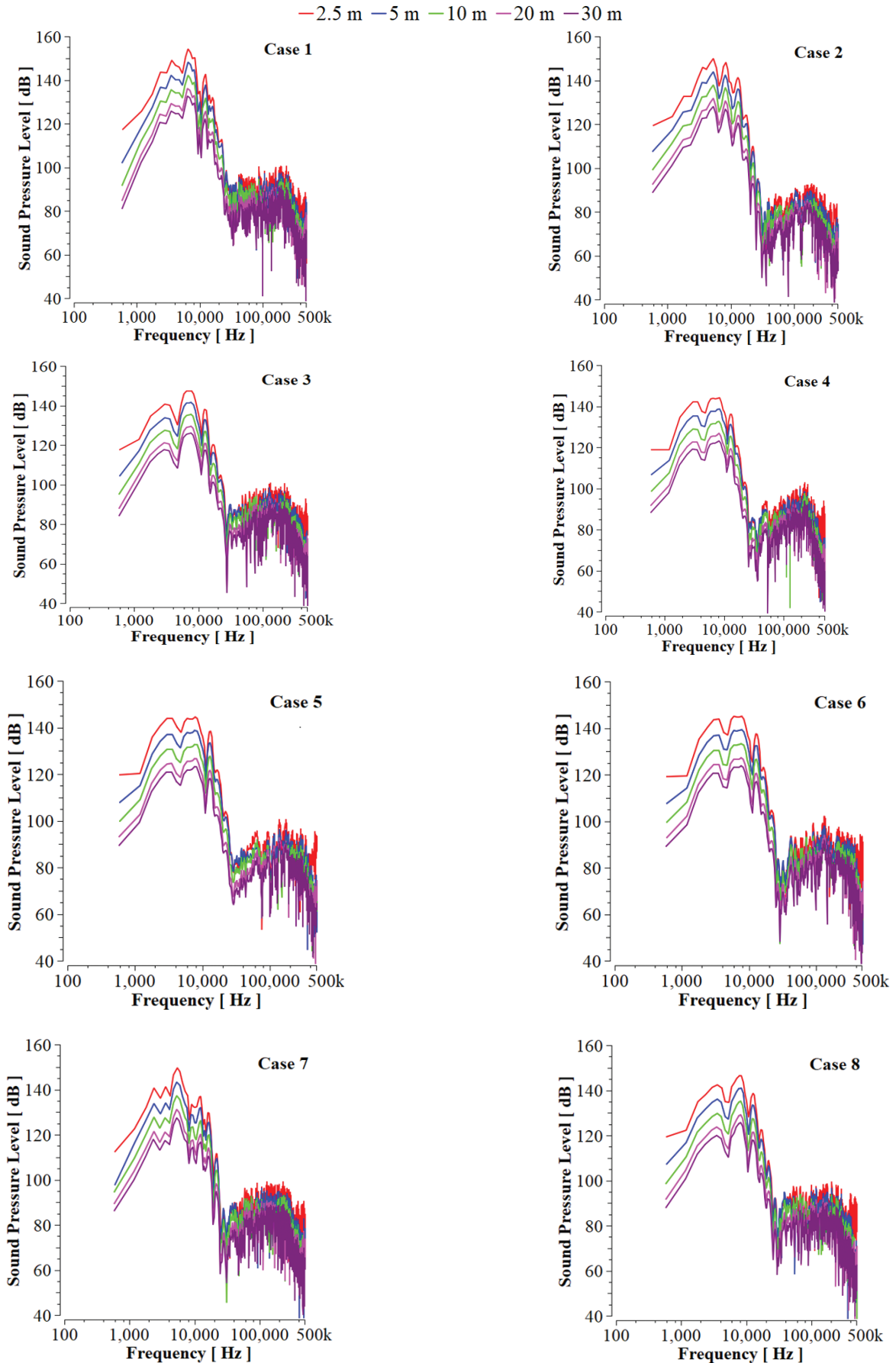
535

Figure 4. Change graphs of SPLs with frequency at different distances.

3. RESULTS AND DISCUSSION

This study aimed to numerically examine the effect of the distance between the baffles and the number of baffles in the suppressor on the SPL$_{peak}$ values occurring in the far field. All analyzes were performed at subsonic projectile velocities throughout the study. The fluent package program, which can solve aeroacoustic and flow field together, was used. Acoustic analysis was carried out using the Ffowcs Williams and Hawkings model. The acoustic pressure signals obtained from this model were post-processed using the Fast Fourier Transform (FFT).

The numerical model was validated by comparing the SPL$_{peak}$ values obtained as a result of firing a 9x19 mm semi-automatic pistol without a suppressor with experimental measurements taken from the study of Gürdamar[23], *et al.* The comparison of experimental and numerical SPL$_{peak}$ values in a 9 mm semi-automatic pistol without a suppressor was given

in Fig. 3. When the numerical and experimental results were compared, the highest error was found to be 1.45 % at a 30 m distance. The evolution of pressure, velocity and temperature distribution in the flow field of the validated model was shown in the study. In the study of Gürdamar[23], *et al.*, the projectile velocity in the barrel exit was measured as 317 m/s. In the numerical model, the projectile velocity at the barrel exit was calculated as approximately 304 m/s. Since the flow during the blast is too complex, the experimental and numerical projectile velocity results showed a slight difference which was about 4 %. Due to the high velocity of the projectile and the limited length of the calculation field, the time step was set to 0.005 ms.

After the numerical model was validated, flow and acoustic analyses of the models with a suppressor were performed. Suppressor models were examined in two configurations according to the arrangement of the baffles. In the first
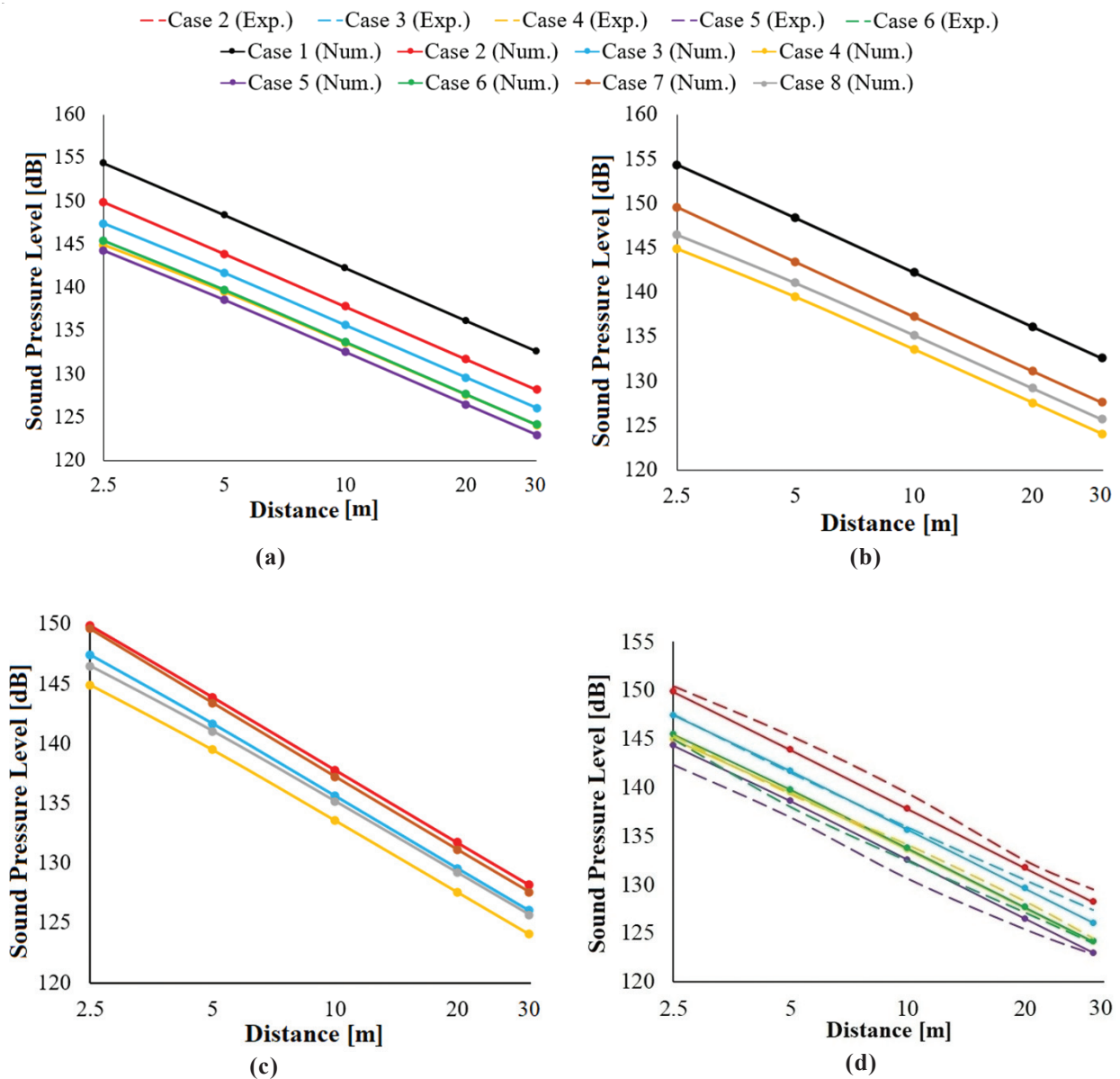

Figure 5. Comparison of SPL$_{peak}$ values at different distances, (a) first configuration cases, (b) second configuration cases, (c) first and second configuration cases, and (d) experimental comparison of first configuration cases.

configuration cases, the baffles were placed in the suppressor at evenly spaced. The number of baffles in the suppressor was determined as 1, 3, 5, 7 and 9. In the second configuration cases, the baffles were placed in the suppressor at 20 mm intervals from the suppressor inlet. The number of baffles in the suppressor was determined as 1, 3 and 5. The obtained SPL_{peak} values were compared within each configuration cases. Then, the two configuration cases were compared with each other.

When the gun is fired, the projectile moves towards the target with the effect of the high-pressure gas in the cartridge. This movement of the projectile triggers the formation of the first precursor shock wave at the barrel exit. A series of compression waves follow this situation. After the air with high pressure and temperature inside the cartridge was ejected from the barrel exit, it expanded radially and formed a typical jet flow structure including bow, barrel, precursor and seconder shock waves. While high pressures occurred in the front field of the jet flow structure, negative pressures occurred in the rear field of the jet flow structure. As the high-pressure air inside the cartridge was strongly discharged from the barrel exit, it interacted with the external ambient and this situation caused the formation of noise. Shock waves at the barrel exit spread over a wider field with time and gradually lost their effect.

As the projectile left the barrel, high-pressure air interacted with the external ambient and high velocities occurred due to the pressure difference behind the projectile. During the period, the velocity behind the projectile continued to increase with time and the highest velocity value was reached at 0.52 ms. In this context, the highest velocity values behind the projectile were in the range of 870-900 m/s at 0.42 ms, 1000-1030 m/s at 0.48 ms and 1010-1040 m/s at 0.52 ms. As the jet flow spread further, it was subjected to friction in the axial direction with the surrounding air, causing the local flow to move in the opposite direction.

The change graphs of SPLs with frequency at different distances were given in Fig. 4. In all graphs, SPL dropped rapidly after peaking in the 5000-8000 Hz frequency range. SPL oscillated roughly in the range of 60-100 dB in the frequency range of 30k-500k Hz in all cases. The SPL_{peak} values decreased as the distance of the receivers increased in all cases. As the number of baffles in the suppressor increased, the zig-zag trend in the frequency ranges where the SPL_{peak} value was obtained decreased.

The comparison of SPL_{peak} values at different distances for the first and second configuration cases as well as the experimental comparison of the first configuration cases, was given in Fig. 5. SPL_{peak} values decreased as the distance to the barrel exit increased in both configuration cases. In the first configuration cases, the highest SPL_{peak} values occurred in case 1, while the lowest SPL_{peak} values occurred in case 5. In case 1, SPL_{peak} values at 2.5 m, 5 m, 10 m, 20 m and 30 m were 154.3 dB, 148.3 dB, 142.2 dB, 136.1 dB and 132.5 dB, respectively. SPL_{peak} values for case 5 at the same distances were 144.2 dB, 138.5 dB, 132.5 dB, 126.5 dB and 122.9 dB, respectively.

When cases 1 and 5 were compared, SPL_{peak} values decreased by roughly 10 dB at all distances. Experimental measurements were carried out for cases 2, 3, 4, 5, 6 and the measurements showed a similar trend with the numerical results. In this context, the highest SPL_{peak} values were obtained in case 2, and the lowest SPL_{peak} values were obtained in case 5. In case 2, the experimental SPL_{peak} values at 2.5 m, 5 m, 10 m, 20 m and 30 m were measured as 150.4 dB, 145.3 dB, 139.4 dB, 132.5 dB and 129.5 dB, respectively. The experimental SPL_{peak} values for case 5 at the same distances
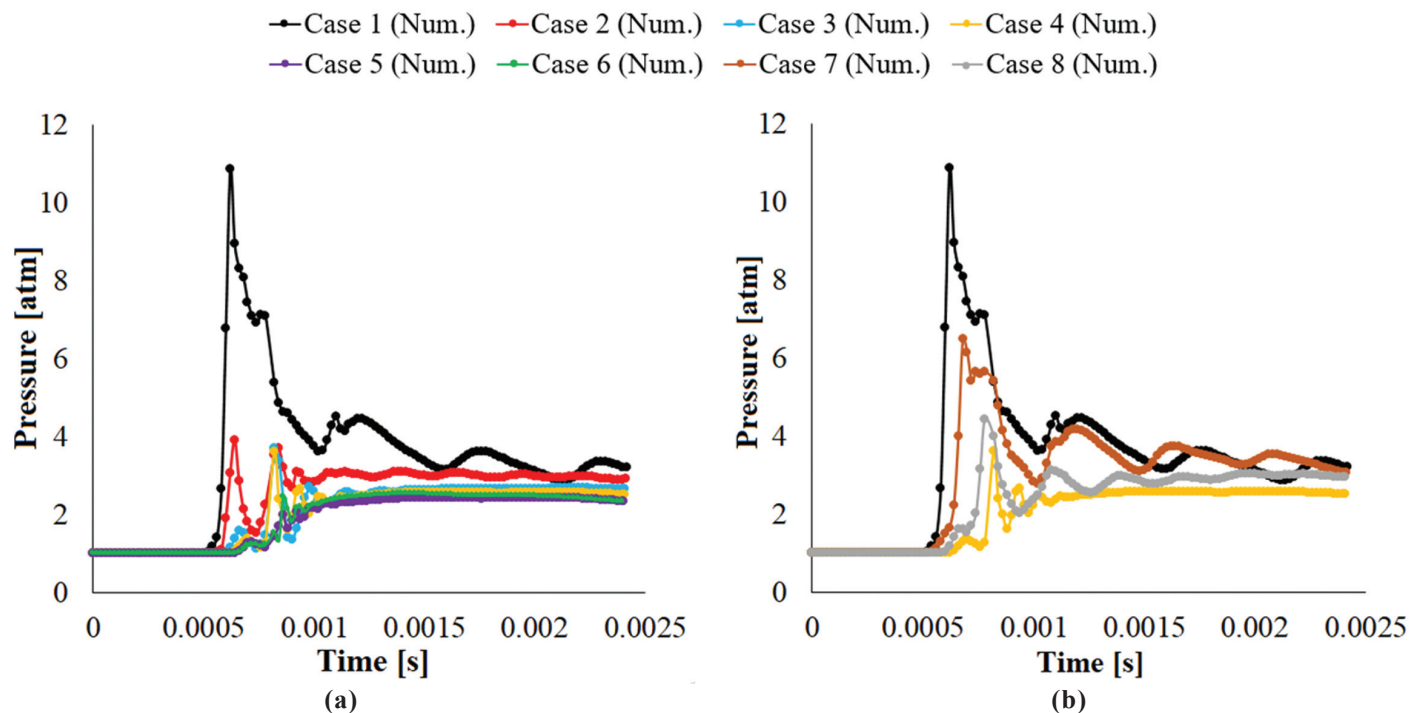

Figure 6. Change graphs of pressure with time at the suppressor outlet. (a) first configuration cases, and (b) second configuration cases.

were measured as 142.3 dB, 136.9 dB, 130.6 dB, 125.4 dB and 122.8 dB, respectively. As a result, the experimental and numerical SPL_{peak} values decreased up to seven baffles in the suppressor and started to increase when more than seven baffles were added to the suppressor. The experimental SPL_{peak} values decreased by roughly 8 dB at all distances when the number of baffles increased from one (case 2) to seven (case 5).

In the second configuration cases, the highest SPL_{peak} values occurred in case 1, as in the first configuration cases. SPL_{peak} values decreased as the number of baffles in the suppressor increased. In this context, the lowest SPL_{peak} values were obtained in case 4, in which SPL_{peak} values at 2.5 m, 5 m, 10 m, 20 m and 30 m were 144.9 dB, 139.5 dB, 133.6 dB, 127.5 dB and 124.0 dB, respectively. When the first and second configuration cases were compared for the same number of baffles, slightly lower SPL_{peak} values were obtained with the baffle arrangement in the second configuration cases.

The change graphs of pressure with time at the suppressor outlet were given in Fig. 6. It took approximately 2.5 ms for the projectile to reach the end of the computation field. In all cases except case 6, the peak pressures decreased as the number of baffles in the suppressor increased. In case 6, the peak pressure at the suppressor outlet increased due to the short distance between the baffles. Moreover, with the increase in the number of baffles, the times at which peak pressures occurred increased. In both configuration cases, the highest peak pressure occurred in case 1 with 10.85 atm in 0.62 ms. In the first configuration cases, the lowest peak pressure in case 5 with 2.43 atm in 1.98 ms. In the second configuration cases, the lowest peak pressure occurred in case 4 with 3.61 atm in 0.82 ms. During the period when the projectile movement was examined, the pressure values at the suppressor outlet oscillated between roughly 2 atm and 4 atm after reaching the peak.

4.   CONCLUSIONS

In this study, the effect of the arrangement of the baffles in the suppressor on the SPL_{peak} was investigated numerically and experimentally. In this context, the number and distance of baffles were changed and totally nine different suppressor models were compared. The main results of this study showed that:

- The projectile's velocity as it exited the barrel was measured experimentally as 317 m/s and calculated numerically around 304 m/s.
- The highest SPL_{peak} errors in the experimental comparison of first configuration cases were calculated as 1.15% for case 2, 1.06% for case 3, 0.56% for case 4, 1.01% for case 5 and 1.26% for case 6.
- Among all cases, the highest and lowest SPL_{peak} values were obtained in cases 1 and 5, respectively. In case 1, the SPL_{peak} values at 2.5 m, 5 m, 10 m, 20 m and 30 m distances were calculated as 154.3 dB, 148.3 dB, 142.2 dB, 136.1 dB and 132.5 dB, respectively. The SPL_{peak} values for case 5 at the same distances were calculated as 144.2 dB, 138.5 dB, 132.5 dB, 126.5 dB and 122.9 dB, respectively.
- The cases with a suppressor having no baffles and without a suppressor showed similar results. However, using a suppressor with no baffle had relatively less noise than the case without a suppressor.
- In the case without a suppressor, the SPL_{peak} value was 156.1 dB at a 2.5 m distance, while this value decreased by nearly 7.6 % in the case of the suppressor with seven baffles which has an average value of 144.2 dB.
- When the first and second configurations were compared for the same number of baffles, the baffle arrangements in the second configuration achieved slightly lower SPL_{peak} values.
- When the first configuration cases were evaluated in terms of peak pressures, the optimum number of baffles was determined as seven. After seven baffles, the peak pressure and, thus, the SPL_{peak} value increased.

This study has brought a methodology to the literature in which flow and acoustic events occurring in firearms can be performed together. In future studies, the effects of different geometries in the suppressor on the SPL_{peak} values can be examined. Moreover, the analyzes in this study can be performed for the three-dimensional computation field, and the results can be compared with this study. Besides, the optimum number of baffles was determined as seven in this study. The SPL_{peak} values were higher at nine baffles case compared to seven baffle case and therefore cases with more than nine baffles were not examined. However, the optimum number may vary in different gun models, different suppressor lengths and baffles with different geometries. For this and similar situations, estimating and optimizing intermediate values, which were not analyzed (for example 2, 4, 6 and 8 baffle cases in this study), with artificial intelligence methodologies will be very valuable in future studies.

REFERENCES

1. Pater, L.; Shea, J. Techniques for reducing gun blast noise levels: An experimental study, 1981, **61**.
2. Zhao, X.Y.; Zhou, K.D.; He, L.; Lu, Y.; Wang, J. & Zheng, Q. Numerical simulation and experiment on impulse noise in a small caliber rifle with muzzle brake. *Shock Vib.*, 2019, 5938034.
   doi: 10.1155/2019/5938034.
3. Pääkkönen, R. & Parri, A. The effect of a suppressor to environmental noise – A case study. *Appl Acoust.*, 2011, **72**, 702–704.
   doi:10.1016/j.apacoust.2011.03.002.
4. Lo, S.W.; Tai, C.H. & Teng, J.T.; Axial-Symmetry Numerical Approaches for noise predicting and attenuating of rifle shooting with suppressors. *J. Appl. Math.,* 2011, 961457.
   doi: 10.1155/2011/961457.
5. Luo, Y.; Xu, D. & Li, H. Analysis of the dynamic characteristics of the muzzle flow field and investigation of the influence of projectile nose shape. *Appl. Sci.,* 2020, **10** (4),
   doi:10.3390/app10041468.
6. Czyżewska, M. & Trębiński, R. Wpływ urządzenia wylotowego lufy na przyrost prędkości pocisku w okresie balistyki przejściowej. Probl mechatronics armament,

Aviat. Saf. Eng., 2015, **6**, 87–98.
doi: 10.5604/20815891.1157779.

7. Jiang, Z. Wave dynamic processes induced by a supersonic projectile discharging from a shock tube. *Phys. Fluids.,* 2003, **15**, 1665–1675.
doi: 10.1063/1.1566752.

8. Kikuchi, Y.; Ohnishi, N. & Ohtani, K. Experimental demonstration of bow-shock instability and its numerical analysis. *Shock Waves,* 2017, **27**, 423–430.
doi: 10.1007/s00193-016-0669-5.

9. Kang, K.J.; Ko, S.H. & Lee, D.S. A study on impulsive sound attenuation for a high-pressure blast flowfield. *J. Mech. Sci. Technol.,* 2008, **22**, 190–200.
doi: 10.1007/s12206-007-1023-8.

10. Xavier, S. Numerical analysis of gun barrel pressure blast using dynamic mesh adaption, embry-riddle aeronautical university dissertations and theses, 2011.

11. Huerta-Torres, J.; Silva-Rivera, U.; Verduzco-Cedeño, V.; Flores-Herrera, L. & Sandoval-Pineda, J. Numerical and experimental analysis of sound suppressor for a 5.56 mm calibre. *Def. Sci. J.,* 2021, **71**.
doi: 10.14429/dsj.71.14957.

12. Hudson, M.; Luchini, C.; Clutter, K. & Shyy, W. The evaluation of computational fluid dynamics methods for design of muzzle blast suppressors for firearms. *Propellants, Explosives, Pyrotechnics*, 2001, **26**, 201-208.
doi: 10.1002/1521-4087(200110)26:4<201::AID-PREP201>3.0.CO;2-7

13. Pääkkönen, R. Environmental noise reduction means of weapons. *J. Acoust. Soc. Am.,* 2008, **123**, 3822.
doi: 10.1121/1.2935577.

14. Rehman, H.; Chung, H.; Joung, T.; Suwono, A. & Jeong, H. CFD analysis of sound pressure in tank gun muzzle silencer. *J. Cent. South Univ. Technol.,* 2011, **18**, 2015–2020.
doi: 10.1007/s11771-011-0936-7.

15. Murphy, W.; Flamme, G.; Campbell, A.; Zechmann, E.; Tasko, S.; Lankford, J., Meinke, D.K.; Finan, D.S. & Stewart, M. The reduction of gunshot noise and auditory risk through the use of firearm suppressors and low-velocity ammunition. *Int. J. Audiol.,* 2018, **57**.
doi: 10.1080/14992027.2017.1407459.

16. Lobarinas, E.; Scott, R.; Spankovich, C. & Le Prell, C. Differential effects of suppressors on hazardous sound pressure levels generated by AR-15 rifles: Considerations for recreational shooters, law enforcement, and the military. *Int. J. Audiol.,* 2016, **55**, 1–13.
doi: 10.3109/14992027.2015.1122241.

17. Nakashima A. A comparison of metrics for impulse noise exposure Analysis of noise data from small calibre weapons, Defence Research and Development Canada Scientific Report DRDC-RDDC-2015-R243, 2015.

18. Bin, J.; Kim, M. & Lee, S. A numerical study on the generation of impulsive noise by complex flows discharging from a muzzle. *Int. J. Numer. Methods Eng.,* 2008, **75**, 964–991.
doi: 10.1002/nme.2291.

19. Lee, I.C.; Lee, D.J.; Ko, S.H.; Lee, D.S. & Kang, G.J. Numerical analysis of a blast wave using CFD-CAA hybrid method. 12th AIAA/CEAS Aeroacoustics Conf. (27th AIAA Aeroacoustics Conf., American Institute of Aeronautics and Astronautics; 2006.
doi: 10.2514/6.2006-2701.

20. Wang, Y.; Jiang, X.H.; Yang, X.P. & Guo, Z.Q. Numerical simulation on jet noise induced by complex flows discharging from small caliber muzzle. *Baozha Yu Chongji/Explosion Shock Waves*, 2014, **34**, 508–512.
doi: 10.11883/1001-1455(2014)04-0508-05.

21. Zhao, X. & Lu, Y. A Comprehensive performance evaluation method targeting efficiency and noise for muzzle brakes based on numerical simulation. *Energies*, 2022, **15**.
doi: 10.3390/en15103576.

22. Murphy, W.J.; Campbell, A.R.; Flamme, G.A.; Tasko, S.M.; Lankford, J.E.; Meinke, D.K.; Finan, D.S.; Stewart, M. & Zechmann, E.L. Developing a method to assess noise reduction of firearm suppressors for small-caliber weapons. *Proc. Meet Acoust.*, 2018, **33**, 40004.
doi: 10.1121/2.0001132.

23. Gurdamar, O.; Ozbektas, S. & Sungur, B. Experimental investigation of the projectile type on sound pressure levels fired with 9 mm gun. *Khazar J. Sci. Technol.,* 2022, **6**(1), 96–104.
doi: 10.5782/2520-6133.2022.6.1.96

24. Ansys User Guide. Fluent, Ver. 18, Ansys Fluent Tutorial Guide. Ansys Inc., Canonsburg, PA, 2017.

CONTRIBUTORS

Mr Onur Gurdamar obtained his MSc degree and working as as R&D Engineer at the Samsun Yurt Savunma company. His areas of research include: Experimental investigations of firearms.
Contribution to the current study: Software, validation, formal analysis, investigation, data curation.

Mr Seyda Ozbektas obtained his MSc degree and working as a Research Assistant at the Mechanical Engineering Department of Ondokuz Mayis University in Samsun, Turkey. His areas of research include: Firearms and numerical investigations of internal and terminal ballistics problems.
Contribution to the current study: Software, validation, formal analysis, investigation, visualisation.

Dr Bilal Sungur received his PhD in Mechanical Engineering from the Ondokuz Mayis University, Samsun, Turkey. He is working as a Assistant Professor at the Mechanical Engineering Department of Samsun University, Samsun, Turkey. His research interests include: Numerical modelling and analysis of firerams.
Contribution to the current study: Conceptualisation, methodology, software, data curation, writing - original draft preparation, supervision.